Natural Resources for Human Health
eISSN: 2583-1194

Original Research

Received 20 April 2026
Revised 14 May 2026
Accepted 16 June 2026

Natural Resources for Human Health 2026, Vol. 6 (3s): 544–561

KEYWORDS:
Retention water, agrochemical release, nitrogen fertilizer, chemical cross-linker, cellulose, methyl cellulose, acrylic acid.

Comparative Study of Cellulose and Methylcellulose Grafted with Acrylic Acid-Based Hydrogels for Enhanced Soil Water Retention and Nitrogen Fertilizer Delivery

[1,2]Akram Waad Nayyef, [2]Fawzi Habeeb Jabrail

[1]Ph.D. Research student in Department of Chemistry, College of Science, University of Mosul, Mosul 41002, Iraq. akraam.24scp21@student.uomosul.edu.iq
[2]Assistant Lecturer at the Scientific Affairs Department, University of Telafer, Iraq. akram@uotelafer.edu.iq
[3]Polymer research laboratory, Department of Chemistry, College of Science, University of Mosul, Mosul 41002, Iraq. fawzijabrail@uomosul.edu.iq

ABSTRACT: Grafting of cellulose (CE) and methylcellulose (MC) with acrylic acid (AA) represent a promising way to enhance soil water retention as well as to transfer fertilizers in a controlled manner to plants. For the purpose of comparison, hydrogels were prepared from cellulose and methylcellulose by grafting them with acrylic acid, (CE-g-AA) and (MC-g-AA). For the purpose of mechanically strengthening them, they were cross-linked with N, N- methylenebisacrylamide (MBA). The following techniques were used to characterize the prepared hydrogels include FT-IR, TGA, XRD, FESEM, and EDS. The degree of swelling of the hydrogels was studied, through which it can determine the suitability of each hydrogel for use in the appropriate place, where the swelling can regulate the loading and releasing behaviors of hydrogel microspheres. As a result, it was observed the (CE-g-AA)/MBA hydrogel, due to its high degree of swelling, is suitable for loading water and help the soil retain water. While (MC-g-AA)/MBA hydrogel, because its swelling is weaker, is suitable for carrying fertilizer, where it was actually loaded with nitrogen fertilizer model KNO3, and its maximum loading percentage (Lmax %) = 19.3%. The study involves studying soil saturation with water and then water retention in soil, where the (CE-g-AA)/MBA hydrogel soil sample has retained water for 19 days compared to 13 days only for controlled sample. The release profile of KNO3-loaded (MC-g-AA)/MBA copolymer hydrogel after choosing three pHs medium for release includes pH 4, pH 7, and pH 9, it was found to be more regular and regulated at pH 7.

INTRODUCTION

The problem of water scarcity, low rainfall, high rate of evaporation and poor soil water-retention capacity in arid and semi-arid regions is a serious one for agricultural production, as crop productivity is reduced and sustainable agriculture is threatened [1,2]. Drought is one of the most destructive environmental stresses for agriculture and causes significant economic losses worldwide [3]. Most of the traditional irrigation methods are inefficient due to the high level of water loss by evaporation and deep percolation, and as a result, inadequate water uses and poor availability of nutrients to plants [4]. Moreover, unstable water supply adversely affects seed germination, plant metabolism, nutrient uptake and overall crop yield [5].

Besides, the excessive use of chemical fertilizers and pesticides with conventional spraying and delivery methods has caused serious environmental concerns. Large quantities of agrochemicals are typically used to compensate for the nutrient losses, which results in soil degradation, pollution of groundwater, toxicity to beneficial microorganisms and earthworms, and long-term ecological imbalance [6,7]. The conventional agrochemical delivery systems also suffer from rapid release and uncontrolled

distribution, which lowers the fertilizer-use efficiency and raises the environmental pollution [8]. Therefore, the development of sustainable systems able to reduce agrochemical consumption and control the release of nutrients has become an important research priority in modern agriculture [9].

Recently, hydrogels have been considered as promising functional materials for agricultural application because of their remarkable ability to absorb, retain and gradually release water [10]. Hydrogels are three-dimensional crosslinked polymeric networks composed of hydrophilic chains that can absorb large amounts of water without dissolving in aqueous environments [11]. These materials increase the water holding capacity of the soil, decrease the frequency of irrigation and improve the water use efficiency especially in drought conditions [12]. Furthermore, hydrogels can act as carriers for fertilizers and pesticides leading to the controlled and sustained release of agrochemicals for long periods [13]. Such controlled-release systems decrease the leaching of nutrients, reduce environmental contamination, and improve the availability of nutrients to plants [14].

Biodegradable hydrogels prepared from natural polymers have recently attracted increasing attention due to their eco-friendly nature, biodegradability, low toxicity and renewability [15]. Cellulose and methyl cellulose, which are among the natural polymers, are considered as highly attractive materials for the preparation of the hydrogel due to their abundance, biocompatibility, hydrophilicity, and excellent swelling properties [10,16]. On the other hand, cellulose-based hydrogels are described as having a lower environmental impact and higher biodegradability than many synthetic hydrogels obtained from petrochemical resources [17].

Cellulose and methyl cellulose are rich in hydroxyl groups, allowing for chemical modification and hydrogel network formation through grafting and crosslinking reactions [18]. Grafting methods are widely used to improve the physicochemical properties, swelling capacity, mechanical strength and controlled-release performance of cellulose-derived hydrogels by grafting natural or synthetic monomers into the polymeric backbone [19]. Cellulose-based hydrogels and their derivatives have been widely studied for biomedical engineering, wastewater treatment, food packaging, tissue engineering and controlled drug delivery systems [15,20]. Cellulose-based hydrogels have shown a great potential as water-retaining materials and controlled-release carriers for fertilizers and pesticides in agricultural applications [2, 12].

The preparation and performance of hydrogels are greatly influenced by the type of crosslinking process used in the synthesis. Crosslinking agents are indispensable to maintain the integrity of the hydrogel structure and to prevent the dissolution or collapse of the polymer network upon water absorption [11]. Besides, crosslinkers are crucial for controlling the release of absorbed water and loaded fertilizers by controlling the porosity and diffusion pathways inside the hydrogel matrix [13]. Therefore, well crosslinked hydrogels can provide a slow and sustained release of water and nutrients, which can improve fertilizer-use efficiency and reduce environment pollution [9].

Hydrogels can be prepared by physical or chemical crosslinking methods. Physical crosslinking depends on non-covalent interactions, such as hydrogen bonding, ionic interactions and crystallization, while chemical crosslinking forms permanent covalent bonds between polymer chains [20]. Crosslinked hydrogels are usually preferred in agricultural applications due to their higher mechanical stability, better swelling resistance and improved controlled-release behaviour [18]. In cellulose based hydrogel synthesis various chemical crosslinkers have been used such as N, N-methylenebisacrylamide (MBA), glutaraldehyde (GA), epichlorohydrin (ECH), citric acid (CA) and sodium hexametaphosphate (SHMP) [19]. MBA is one of the most used crosslinkers due to its high efficiency in the formation of stable polymeric networks, while SHMP has received attention as a relatively safer and environmentally friendly crosslinker for biodegradable hydrogel systems [20].

In this study, two biodegradable hydrogels were successfully prepared from cellulose (CE) and methyl cellulose (MC) as natural polymeric matrices, grafted with acrylic acid (AA) and chemically cross-linked with N, N'-methylenebisacrylamide (MBA). The prepared hydrogels (CE-g-AA)/MBA and (MC-g-AA)/MBA were loaded with potassium nitrate (KNO_3) as nitrogen fertilizer model and then studied for their release behavior in different pH environments, as well as their capability for water retention over a long period.

Experimental

MATERIALS AND METHODS

Cellulose (CE) was obtained from CelluTech Pharma Pvt. Ltd., Gujarat, India, and methyl cellulose (MC) was purchased from Shandong Head Co., Ltd., Meihua Group, China. Acrylic acid was supplied by Sigma Aldrich, and NaOH, as well as N, N'-

methylenebisacrylamide (MBA), ammonium persulfate (APS), and potassium nitrate (KNO_3), were supplied by BDH, UK. Buffered solutions, including different pH solutions were purchased from Fluka, Switzerland.

Preparation of (CE-g-AA)/MBA hydrogel

Cellulose (5.0 g) was dissolved in 100 mL of 0.1 M NaOH and transferred into a 500 mL three-necked flask. The flask was fitted with a mechanical stirrer, a reflux condenser, a thermometer, and a nitrogen line to provide inert nitrogen for the reaction. Alkaline pyrogallol solution was used in the nitrogen line to remove any remaining oxygen. The CE solution was heated to 60°C for 1.0 hour to form a colloidal slurry. Then 30 mL of a 5% w/v APS aqueous solution was added, and the mixture was stirred continuously for 15.0 min. In a separate flask, 35.0 mL of acrylic acid (AA) was neutralized with 8.0 M NaOH solution, and 4.0 g of cross-linker MBA was mixed together and then added dropwise to the three-necked flask while stirring. The temperature of the final solution was raised gradually to 70°C and maintained for 3.0 hours with stirring and under nitrogen gas to complete grafting. The hydrogel, after preparation was cleaned and dried.

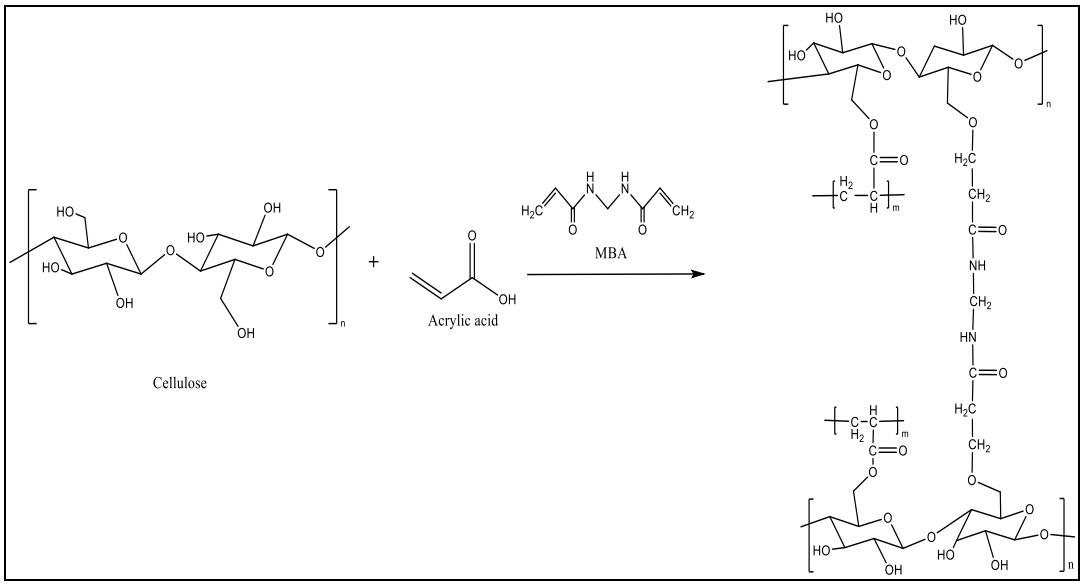

Scheme 1: Preparation and chemical structure of (CE-g-AA)/MBA hydrogel

Preparation of (ME-g-AA)/MBA hydrogel

Methyl cellulose (MC) (5.0 g) was dissolved in 100 mL of 0.05 M NaOH and transferred into a 500 mL three-necked flask. The flask was fitted with a mechanical stirrer, a reflux condenser, a thermometer, and a nitrogen line to provide inert nitrogen for the reaction. Alkaline pyrogallol solution was used in the nitrogen line to remove any remaining oxygen. The MC solution was heated to 60°C for 1.0 hour to form a colloidal slurry. Then 30 mL of a 5% w/v APS aqueous solution was added, and the mixture was stirred continuously for 15.0 min. In a separate flask, 35.0 mL of acrylic acid (AA) was neutralized with 8.0 M NaOH solution, and 4.0 g of cross-linker MBA was mixed together and then added dropwise to the three-necked flask while stirring. The temperature of the final solution was raised gradually to 70°C and maintained for 3.0 hours with stirring and under nitrogen gas to complete grafting. The hydrogel, after preparation, was cleaned and dried.

Natural Resources for Human Health
eISSN: 2583-1194

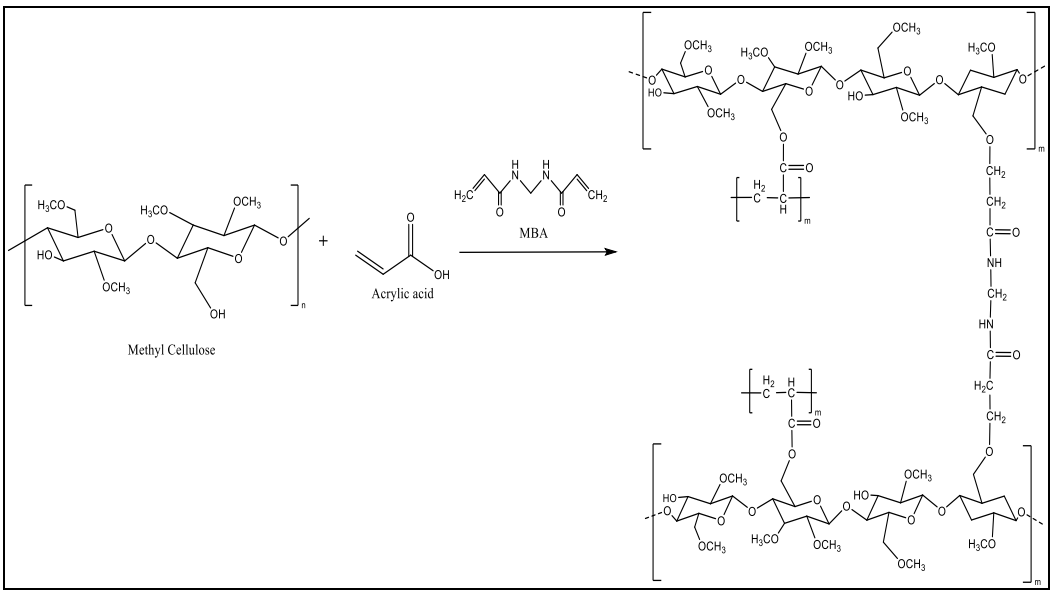

Scheme 2: Preparation and chemical structure, of the (MC-g-AA)/MBA hydrogel

Study the degree of swelling

The prepared hydrogels were studied for their degree of swelling in two environments, including distilled water and rainwater, as well as at three different temperatures. Hence, 1.0 g of dry microspheres were immersed in 100 mL distilled water or 100 mL of rainwater. The change in their degree of swelling was detected by measuring the increase in their weights every 3.0 hours until their weights remained constant and their maximum degree of swelling was reached. The experiment was conducted at three different temperatures including 5°C, 25°C, and 45°C, and the degree of swelling was calculated according to the following equation [21]:

$$DS(\%) = \frac{w_t - w_o}{w_o} \times 100 \ldots\ldots\ldots\ldots\ldots\ldots 1$$

Where w_t and w_o represent the weights of swelling microspheres at time (t) and their dry weights, respectively.

Loading measurements

The findings of the degree of swelling measurements for the manufactured hydrogels showed that the loading study will involve two separate substances one being water and the other being agrochemical (KNO_3).The reason for using different substances is due to the different degrees of swelling for the prepared hydrogels; therefore, we carried out an experiment with water loading for (CE-g-AA)/MBA and potassium nitrate for (MC-g-AA)/MBA.

The loading study of agrochemicals such as KNO_3 fertilizer is performed using two formulae: maximum loading percentage (Lmax %) and loading efficiency percentage (EL%). A (100 mg) hydrogel microsphere was immersed in (100 ml) loading solution produced from phosphate buffered solution (pH 7) containing (200 mg) potassium nitrate (KNO_3) fertilizer. The microspheres were immersed in the loading solution for (24 h) at room temperature and under moderate stirring. A calibration curve for KNO_3 must be created in advance in order to calculate unknown concentrations of the fertilizer. KNO_3 was prepared with known quantities of 25 mg, 50 mg, 75 mg, 100 mg, 125 mg, and 150 mg in 100 ml of phosphate- buffered solution (pH 7). The wavelength of KNO_3 at maximum absorbance (λmax) was determined using a UV-visible spectrophotometer type JASCO V- 630, Tokyo, Japan. The UV instrument was adjusted to the λmax of KNO_3 (298 nm), and then the absorbance (A) of the known concentrations of KNO_3 was measured. Finally, plotting the obtained absorbance (A) against their concentrations (g/dL) will produce the calibration curve of KNO_3 fertilizer [12].

The hydrogel microspheres were immersed in the KNO_3 loading solution for a prescribed duration, filtered using a fine mesh sieve (100 meshes), and left to drain for an additional 10 minutes. Finally, the concentration of the loaded KNO_3 was indirectly obtained by collecting a few milliliters of the leftover loading solution and measuring its absorbance (A) at λmax=298 nm using

a UV-visible spectrophotometer. The fertilizer loading calculation is performed based on the following equations using two formulas: maximum loading percentage Lmax (%) and loading efficiency percentage EL (%) [22]:

.

$$\text{Lmax (\%)} = \frac{\text{Weight of } agrochemical \text{ loaded(mg)}}{\text{Weight of microspheres taken for loading (mg)}} \times 100 \text{.....2}$$

$$\text{EL (\%)} = \frac{\text{weight of agrochemical loaded (mg)}}{\text{weight of agrochemical taken for loading (mg)}} \times 100 \text{ ... ... 3}$$

Study of release

Release behavior of KNO_3 fertilizer-loaded hydrogel microspheres was investigated. Generally, 100 mg of KNO_3 -loaded microspheres were placed in 20 ml of buffered solution at pH 4, 7, and 9, where pH 4 reflects a very acidic state that can be found in rainy areas with acid sulfate soils. pH 9, on the other hand, is characteristic of alkaline soils occurring in dry and semi-arid environments, while pH 7 is the neutral pH of most agricultural soils. The release of KNO_3 from hydrogel microspheres was conducted at 45°C utilizing a water bath in rainwater. The release of KNO_3 from the hydrogel microspheres was determined at 2hour intervals by measuring, the absorbance (A) of KNO_3 at its characteristic wavelength (λmax=298 nm) using a UV–visible spectrophotometer. A 3 mL aliquot of the release medium was removed, absorbance was measured and it was replaced in the media. The controlled release (CR_{max}%) of fertilizer was calculated using equation 4 [12, 23, 24]:

$$\text{Controlled release (CRmax) \% } = \Sigma \left(\frac{W_t}{W_0} X100\right) constant \text{.....4}$$

Burst release (BR_{max}%) was calculated using equation 5 [24]:

$$\text{Burst release (BRmax) \% } = \Sigma \left(\frac{W_t}{W_0} X100\right) variable \text{.....5}$$

The overall agrochemical release was calculated as cumulative release $(\text{Rcum\%})$ using equation 6 [25]:

$$\text{Cumulative release (Rcum)\%} = \frac{W_t}{W_0} \times 100 \text{ .....6}$$

Where W_t is the cumulative quantity of KNO_3 released at time (t) and W_0 is the entire amount of KNO_3 released.

Degree of saturation of soil measurement

A sample of agricultural soil was gathered from agricultural fields in Mosul, cleansed of contaminants, and sieved. A 150 g sample of cleansed soil was placed in a paper cup with a bottom punctured by a suitable number of very fine holes. Rainwater was added to the cup carefully, continuing to add until the water drained from the bottom of the cup.

The wet soil was weighed to the nearest quarter of a gram and dried in an oven at 102°C for 24 hours. The dry soil cup was allowed to cool outside the oven for 1 hour and then weighed. The weight of the soil was obtained by subtracting the weight of the cup from the total weight of the cup with soil, and the degree of saturation was determined by the following equation [26]:

$$Degree\ of\ saturation\ \left(\frac{g}{g}\right) = \frac{W_2 - W_1}{W_1 - W_0} \text{.....7}$$

Where W_2 represents the total weight of wet soil at saturation, W_1 is the weight of dry soil out of the oven, and W_0 represents the original weight of the soil sample.

Water retention measurement of the hydrogels

The water retention percentage of (CE-g-AA)/MBA hydrogel was measured. A sample of 200 g of dry soil in a paper cup was prepared, and 1.0 g of dry hydrogel was placed at a depth of one centimeter from the surface of the soil in the cup. The degree of saturation was analyzed and the amount of rainwater to be added to the soil is computed. A controlled cup sample was prepared with the same elements and conditions as the previous one, except with no hydrogel. At the time of investigation, the soil-hydrogel cup, beside the controlled cup, was maintained at room temperature and at appropriate air humidity, but not more

than 25 %. The cups were weighed daily and recorded and finally, the water retention percentage was estimated using the following equation [27]:

$$Water\ retention\ (\%) = \frac{Wt}{Wo} \times 100 \quad \ldots\ldots\ldots\ldots\ldots 8$$

Where Wt represents the daily decrease in the cup weight, while Wo represents the initial weight of the cup.

Results and Discussion

The foundation of agricultural fields is the attention of agriculture to the processing of nutritional materials for plants, such as fertilizers and water. Thus, hydrogels are capable of realizing a variety of significant uses. The hydrogels CE-g-AA/MBA and MC-g-AA /MBA were made and cross-linked by the identical cross-linkers. They were employed to deliver water and potassium nitrate (KNO_3) fertilizer to the plants in a regulated manner.

Characterization of hydrogels

FT-IR Spectroscopy

The FT-IR spectrum of (CE-g-AA)/MBA hydrogel is shown in Fig. 1. Distinctive frequencies (Table 1) of the hydroxyl group and $\upsilon(N\text{-}H)_{str}$ in amide groups are seen at 3187 cm^{-1}. Of course, the hydrogel comprises amide groups present as amide I ($\upsilon(C{=}O)_{str}$) and amide II ($\delta(N\text{-}H)_{bent}$ and $\upsilon(C\text{-}N)_{str}$) at 1696 cm^{-1} and 1538 cm^{-1}, respectively. Further, the absorption frequency at 1387 cm^{-1} corresponding to $\delta(C\text{-}O\text{-}H)_{bend}$ is due to the poly (CE-g-AA)/MBA polymer. The hydrogel (MC-g-AA)/MBA displays absorption frequencies (Fig. 2 and Table 1) at 3359-3294 cm^{-1}, which are assigned to hydroxyl and amide groups.

Table 1: FT-IR characteristic frequencies of the main functional groups of the prepared hydrogels

Hydrogel	$\nu(O\text{-}H)_{str}$	$\nu(C\text{-}H)_{str}$ Aliph.	$\nu(C{=}O)_{str}$	$\nu(N\text{-}H)_{str}$	$\nu(C{=}O)_{str}$ Asym/sym	$\nu(C\text{-}O)_{str}$	$\nu(C\text{-}N)$ bending	$\delta(C\text{-}OH)$ def
	Wave number υ/cm-1							
(CE-g-AA)MBA	3187	2994 2948	1696	1538	1410	1060	1149	1387
(MC-g-AA)MBA	3359 3294	2939 2840	1637	1545	1360	1059	1112	1315

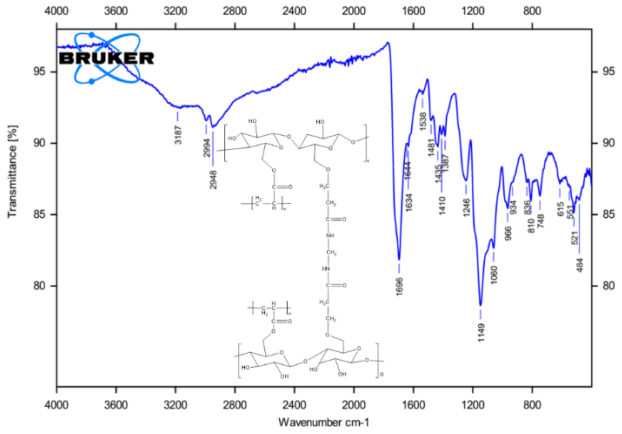

Figure 1: FT-IR spectrum of (CE-g-AA)/MBA hydrogel

Natural Resources for Human Health
eISSN: 2583-1194

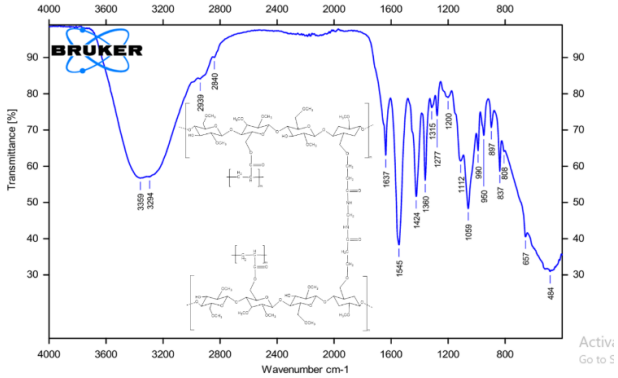

Figure 2: FT-IR spectrum of (MC-g-AA)/ MBA hydrogel

^{1}H NMR Spectroscopy

^{1}H NMR spectrum of (CE-g-AA)/MBA hydrogel (Fig. 3) and its chemical shifts (Table 2) have exhibited proton resonance (2H, s) at 1.32 ppm for the methylene (-CH_2-) group of AA and MBA and 1.58 ppm for the methine (>CH-) group of CE and AA, besides 2.29 ppm for the methine (>CH-C=O) groups of AA. The resonance at 2.37 ppm is of the (-OH) group of cellulose, and at 4.82 ppm is of (-CH_2-O-C=O), which is the connection between CE and AA. The proton resonance at 4.84 ppm (2H, m) corresponds to methylene (-CH_2-O-CH_2-), which is indicative of the linkage between CE and the MBA. The secondary amide group (-NH) of MBA is also observed at 7.28 ppm. Finally, the ^{1}H NMR spectra, including their chemical shifts (Fig. 3 and Table 2), confirm the chemical structure of CE-g-AA/MBA hydrogel.

Table 2: ^{1}H NMR chemical shifts of the manufactured hydrogels

Hydrogel	Chemical Shift δ/ppm	Description of protons
(CE-g-AA)/MBA	1.320	(2H, s) of methylene (−CH_2 −) group of AA, and MBA
	1.580	(1H, s) of methine (> CH −) group of CE, and AA
	2.290	(1H, m) of methine (> CH-C=O) group of AA
	2.370	(1H, m) of (−OH) group of CE
	4.820	(2H, m) of (-CH_2-O-C=O) connection between CE, and AA
	4.840	(2H, m) of (-CH_2-O-C=O) connection between CE, and MBA
	7.280	(1H, m) of (−NH) secondary amide of MBA
(MC-g-AA)/MBA	0.850	(1H, m) of methine (> CH −) group of MC, and AA
	1.270	(2H, m) of methylene (−CH_2 −) group of AA, and MB
	2.790	(1H, m) of (−OH) group of MC
	2.750	(1H, m) of (> CH-C=O) group of AA
	3.660	(3H, s) of (−OCH_3) group of MC
	4.450	(2H, s) of (−OCH_2 −) group of MC
	4.800	(2H, s) of (-CH_2-O-CH_2) connection between MC, and MBA
	7.240	(1H, s) of (−NH) secondary amide of MBA

Natural Resources for Human Health
eISSN: 2583-1194

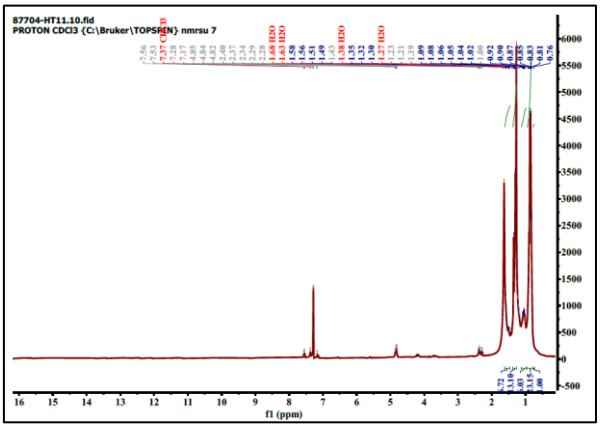

Figure 3: ^{1}H NMR spectrum of (CE-g-AA)/MBA hydrogel

The copolymer hydrogel (MC-g-AA)/MBA has shown a ^{1}H NMR spectrum (Fig. 4) and chemical shifts (Table 2). It is improved (MC-g-AA)/MBA with the following details: a methine (>CH-) group at 0.85 ppm present in MC and AA and a methylene (-CH_2-) group at 1.27 ppm, which belongs to AA and MBA. The (-OH) groups of the MC polymer are observed at 2.79 ppm, and methine (>CH-C=O) groups of AA appear at 2.75 ppm. The proton resonances (3H, s) and (2H, s) of the (-OCH_3) and (-OCH_2-) groups of the MC polymer appeared at 3.66 ppm and 4.45 ppm, respectively. The methylene (-CH_2-O-CH_2-) groups, at 4.80 ppm, represent the linkage between MC and MBA. The secondary amide (-NH) group of MBA appeared at 7.24 ppm. All these chemical shifts (Fig. 4 and Table 4.6) demonstrate that the measured molecule is an (MC-g-AA)/MBA hydrogel.

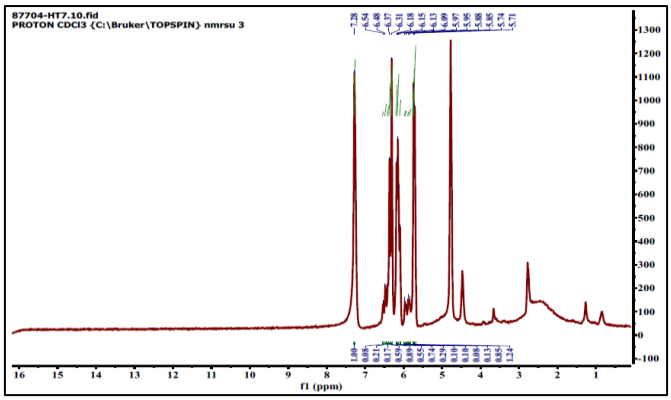

Figure 4: ^{1}H NMR spectrum of (MC-g-AA)/MBA hydrogel

Thermal Analysis

The thermal stability of the synthesized copolymer hydrogels has been studied. Their thermogravimetric analysis (TGA) and differential scanning calorimetry (DSC) have been evaluated. The data are recorded in Table 3.

Table 3: TGA and DSC thermal analysis data of the hydrogels

Hydrogel	TGA weight loss (%)				DSC (w/g)	
	IDT °C	FDT °C	T_{max} °C	T_{Cr} °C	Tg °C	ΔH (j/g)
(CE-g-AA)/MBA	1.9 35.5 °C	76.2 603.5 °C	38.0 225.0 °C	72.5 431.5 °C	48.0	+562.5+113.3+30.3 35.1 °C 373.1 °C 448.1 °C

(MC-g-AA)/MBA	0.40 54.2 °C	47.2 613.0 °C	24.5 420.5 °C	44.0 509.5 °C	70.5	+411.8+103+135.1+42.8 77.3 °C 139.9 °C 318.4 °C 488.4 °C

The TGA thermogram of the (CE-g-AA)/MBA hydrogel (Fig. 5) and its data (Table 3) showed that the hydrogel is thermally stable, with a weight loss of 1.9% at 35.5°C (IDT) and 76.2% at 603.5°C (FDT). Also, the weight loss at T_{max} is 38.0% at 225.0°C, while the weight loss at T_{Cr} is 72.5% at 431.5°C. The DSC thermogram (Fig. 5 and Table 3) indicated that the hydrogel has Tg = 48.0°C and exhibits three different endothermic heat fusion (ΔH) curves of +562.5 J/g, +113.3 J/g and +30.3 J/g at 35.1°C, 373.1°C and, 448.1°C, respectively. The (CE-g-AA)/MBA hydrogel is thermally stable, compact, and mechanically strong due to covalent bonding and hydrogen interactions [28].

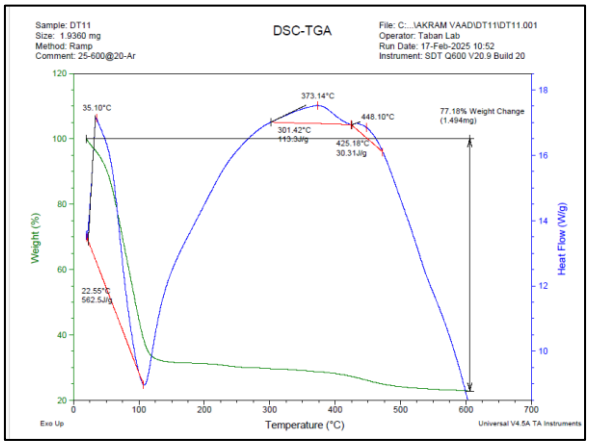

Figure 5:TGA and DSC thermogram of (CE-g-AA)/MBA hydrogel

The TGA thermogram of (MC-g-AA)/MBA copolymer hydrogel (Fig. 6) and its data (Table 3) indicate that the hydrogel is thermally stable with a weight loss of 0.40% at 54.2°C (IDT) and a weight loss of 47.2% at 613.0°C (FDT). Also, the weight loss at Tmax is 24.5% at 420.5°C, while the weight loss at T_{Cr} is 44.0% at 509.5°C. Moreover, the DSC thermogram (Fig. 6 and Table 3) shows that the hydrogel has Tg = 70.5°C and offers four different endothermic heat fusion (ΔH) curves of +411.8 J/g, +1.3 J/g, +135.1 J/g, and +42.8 J/g at 77.3°C, 139.9°C, 318.4°C, and 488.4°C, respectively. All studies indicate that the synthesized hydrogel (MC-g-AA)/MBA is thermally stable, has outstanding mechanical strength and a dense, compact network [29].

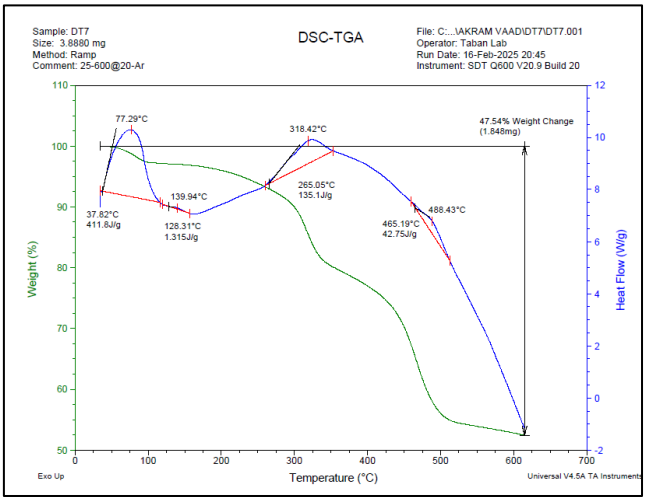

Figure 6:TGA and DSC thermogram of (MC-g-AA)/MBA hydrogel

XRD diffraction

The XRD pattern of (CE-g-AA)/MBA copolymer hydrogel (Fig. 7) indicates that the generated hydrogel is amorphous in nature, even though cellulose is one of its constituents, as the cross-linker MBA has the ability to reduce the crystallinity of cellulose. MBA may disrupt the successful packing of cellulose molecules and the cellulose chains are locked in a 3D network, preventing the production of hard, crystalline domains [30].

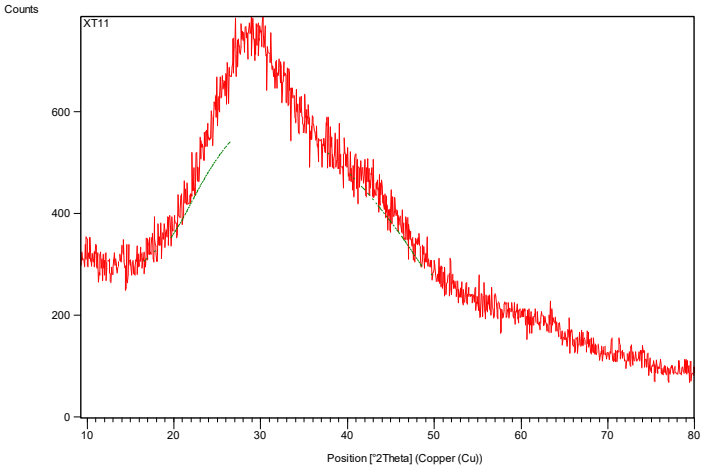

Figure 7: XRD pattern of (CE-g-AA)/MBA hydrogel

The XRD pattern of (CE-g-AA)/MBA copolymer hydrogel (Fig. 8) demonstrates that the produced hydrogel is amorphous in nature, with one crystalline peak at 22.46° along the 2θ axis representing the methyl cellulose peak, which has a semi-crystalline or nearly amorphous nature because of the disruption of the cellulose structure during the methylation process [31]

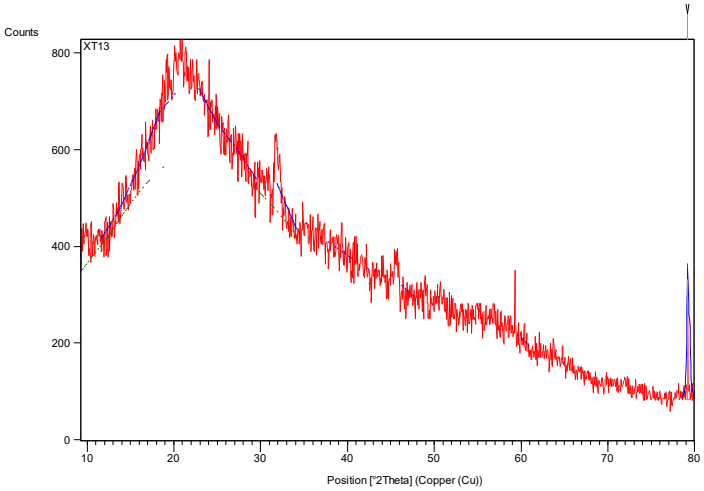

Figure 8: XRD pattern of (MC-g-AA)/MBA hydrogel

BET analysis

An essential way to characterize the porous structure of hydrogel microspheres is by Brunauer-Emmett-Teller (BET) analysis, especially for hydrogels employed in applications that need a large surface area, such as drug administration, agrochemical release, desorption, and tissue engineering. Thus, the main measures of surface area, pore size, and its volume are quantitative, and BET may provide them.

The BET analysis data of (CE-g-AA)/MBA and (MC-g-AA)/MBA hydrogels (Table 4) show that their BET data are very close because the two hydrogels are almost similar; the only variation is that one hydrogel uses cellulose and the other uses methyl cellulose, and both are chemically cross-linked and have a compact network. The BET plot data (Table 4) reveal that the specific surface area (as) of (MC-g-AA)/MBA is the highest, whereas the total pore volume and average pore diameter of (CE-g-AA)/MBA hydrogel are greater, which means (MC-g-AA)/MBA hydrogel is physically described as a dense, tightly cross-linked or possibly nanoporous network [32].

The (CE-g-AA)/MBA hydrogel is physically characterized by a coarse and open-network structure with extensive internal spaces [33].

Table 4: BET analysis data of (CE-g-AA)/MBA, and (MC-g-AA)/MBA hydrogels

Plot		Hydrogel	
type	**data**	**(CE-g-AA)/MBA**	**(MC-g-AA)/MBA**
		Adsorption result	
BET	Vm	$3.4116[cm^3(STP)^{-1}]$	$4.1573[cm^3(STP)g^{-1}]$
	as, BET	$14.849[m^2g^{-1}]$	$18.095[m^2g^{-1}]$
	Total pore volume	$0.0666[cm^2g^{-1}]$	$0.0562[cm^3g^{-1}]$
	Average pore diameter	17.933[nm]	$12.43[nm]$
Lang	Vm	$4.9711[cm^3(STP)^{-1}]$	$3.9664[cm^3(STP)g^{-1}]$
	as, Lang	$21.636[m^2g^{-1}]$	$17.264[m^2g^{-1}]$
	B	0.3354	1.6017
BJH	Vp	$0.0689[m^2g^{-1}]$	$0.0545[m^3g^{-1}]$
	rp, peak (Area)	5.32[nm]	5.32[nm]
	Ap	$18.765[cm^2g^{-1}]$	$10.449[m^2g^{-1}]$

The Langmuir plot data (Table 4) demonstrates that (CE-g-AA)/MBA hydrogel has great structural stability and delivers adjustable porosity [34]. The total pore area of (CE-g-AA)/MBA hydrogel in the BJH plot (Table 4) is highest, signifying that (CE-g-AA)/MBA hydrogel is more compact.

FESEM and EDX/EDS Analysis

The FESEM image of (CE-g-AA)/MBA hydrogel (Fig. 9) indicates that the surface of the hydrogel is uniform and compact. The hydrogel appears to have a solid texture, with a coarse surface and no pores. The addition of cellulose increases the network stability and enables larger swelling, and the hydrogel will acquire good superabsorbent properties with a high degree of swelling [35].

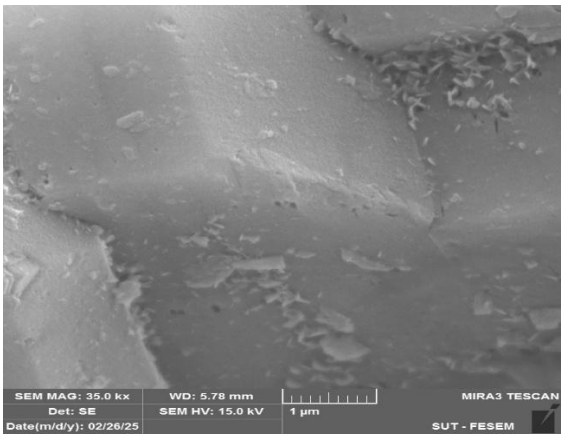

Figure 9: FESEM image of (CE-g-AA)/MBA hydrogel

The FESEM image of (MC-g-AA)/MBA hydrogel (Fig. 10) indicates that the morphology of the hydrogel consists of clusters of blocks with compact structure, featuring a folds and holes. Characterizations of the hydrogel show that it can load a high quantity of materials.

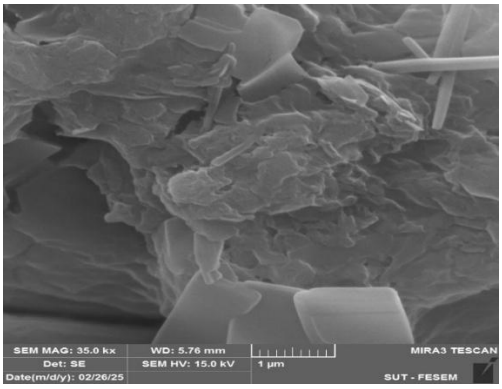

Figure 10: FESEM image of (MC-g-AA)/MBA hydrogel

EDX/EDS Analysis

Energy dispersive X-ray spectroscopy (EDX/EDS) study is an important characterization technique for hydrogels, providing information on their chemical composition and structural integrity.

The EDS charts and tables of (CE-g-AA)/MBA and (MC-g-AA) /MBA hydrogels (Figs. 10-11) indicate mainly carbon and oxygen elements.

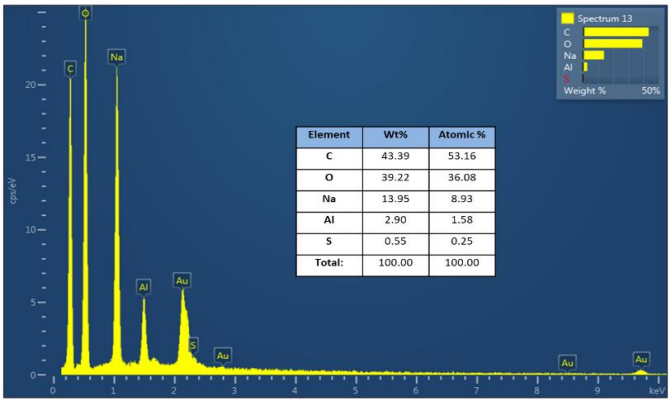

Figure 11: EDS OF (CE-g-AA)/MBA hydrogel

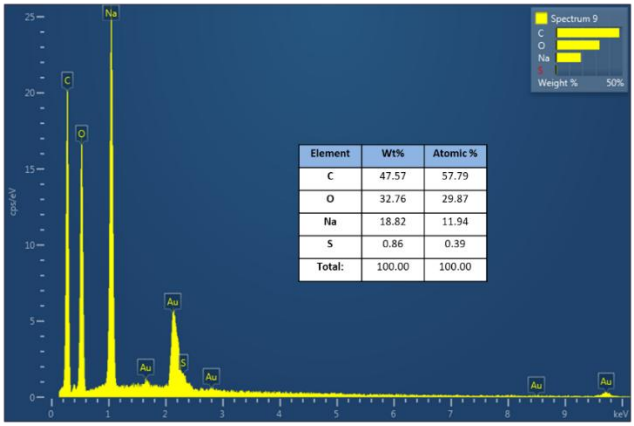

Figure 12: EDS OF (MC-g-AA)/MBA hydrogel

Natural Resources for Human Health
eISSN: 2583-1194

Studies degree of swelling

The swelling behaviors of hydrogel microspheres should be measured. The swelling can regulate the loading and releasing behaviors of hydrogel microspheres.

DS% of (CE-g-AA)/MBA and (MC-g-AA)/MBA hydrogels in distilled water (Fig. 13 a).

The maximum DS of hydrogel (CE-g-AA)/MBA was in distilled water at 25°C (Fig. 13 a). The maximum swelling capacity depends on the acrylic acid concentration and the cross-linking density of MBA.

The grafted AA chains have hydrophilic groups (-C00-) and (-C00H) that absorb water well, and the cellulose backbones provide structural integrity [36]. (Fig. 14 a) shows the DS % of (CE-g-AA)/MBA hydrogel in rainwater swelling media reached highest at 5°C, which is attributed to less kinetic energy resulting in slower, more network expansion in cool environmental conditions. The highest swelling is attained in slightly acidic nature or rainwater, as there is an optimal balance between osmotic pressure and network rigidity, which enables the polymer to reach its maximum swelling [37].

The DS% of (MC-g-AA)/MBA copolymer hydrogel was determined in distilled water (Fig. 13b), and its maximum was attained at 45°C due to the balance between water diffusion and structural integrity. However, the rise in temperature up to 45°C in distilled water can improve water absorption by enhancing the expansion of the hydrogel network. Therefore, the greatest swelling capacity of the hydrogel is attained when the osmotic pressure differential between the gel and the distilled water is at maximum [38].

The DS% of (MC-g-AA)/MBA hydrogel determined in rainwater (Fig. 14b) was greatest at 25°C due to its low ionic strength, which caused complete ionization of the (-C00H) groups on the acrylic acid chain, causing maximal electrostatic repulsion. It is established that 25°C is considered the generally ideal ambient temperature for swelling in low-salt media such as rainwater or distilled water. Finally, the ionization of the common (-C00H) groups in rainwater is neutralized, maximizing repulsion and porosity, which increases owing to grafting that facilitates quick water absorption [37].

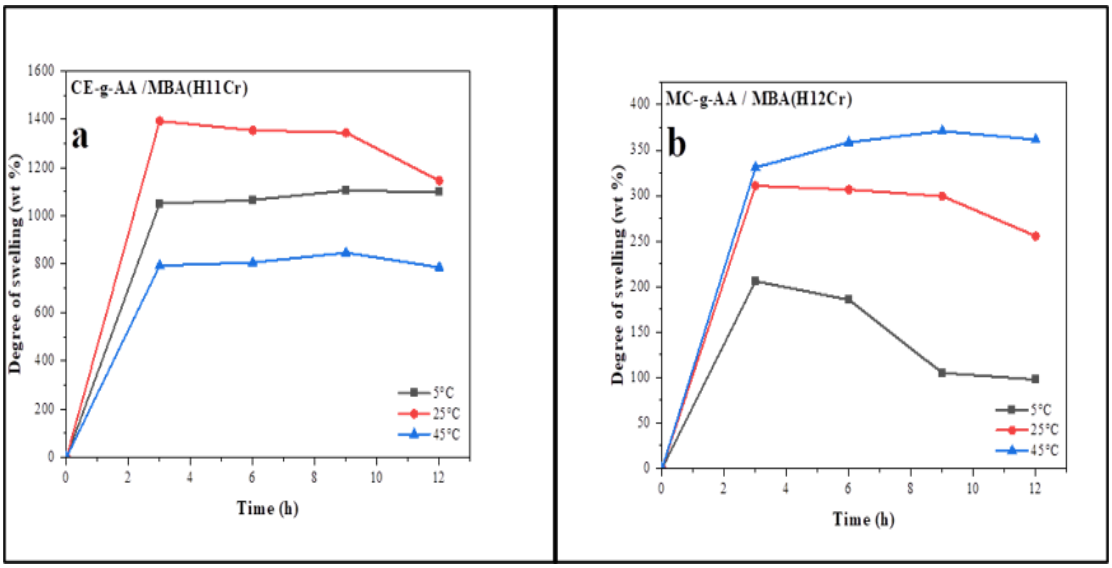

Figure 13: DS % of (CE-g-AA)/MBA and (MC-g-AA)/MBA copolymer hydrogel in distilled water at different temperature.

Natural Resources for Human Health
eISSN: 2583-1194

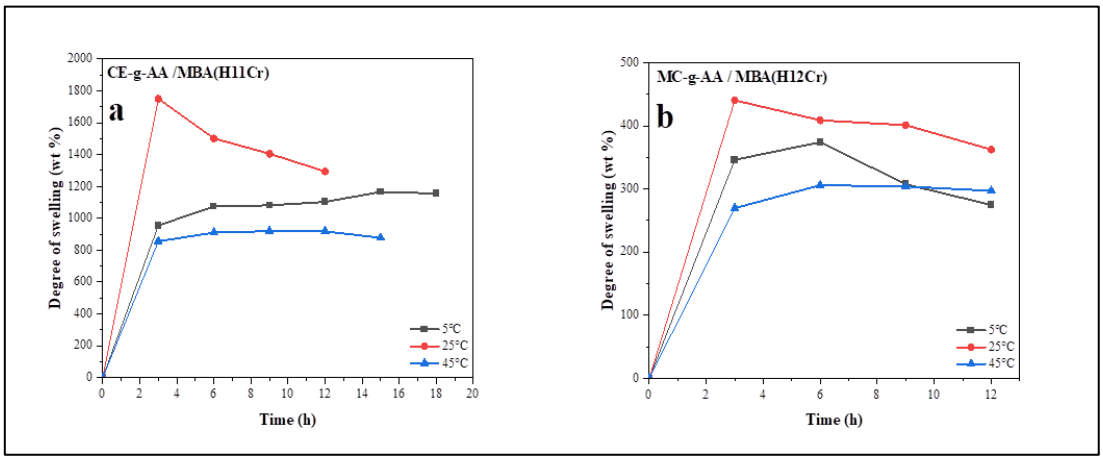

Figure 14: DS % of (CE-g-AA)/MBA and (MC-g-AA)/MBA copolymer hydrogel in rainwater at different temperature.

Loading into hydrogel microsphere.

Same cross-linkers produced hydrogels exhibit varying degrees of swelling even with different loading contents (agrochemical and water). Thus, the maximum loading percentage of agrochemical, such as potassium nitrate, in the (MC-g-AA)/MBA is studied due to its reduced degree of swelling, while water for (CE-g-AA/MBA) is selected because of its high degree of swelling.

The study of maximum loading percentage (Lmax %) and efficiency loading percentage for (MC-g-AA)/MBA shows that the maximum loading of (MC-g-AA) / MBA exhibits a very low Lmax (%) of 19.3% (Table 5) due to the hydrogel's limited network swelling capacity and low degree of grafting of acrylic acid on methylcellulose, which results in low grafting efficiency. In addition, there is usually a competitive homo-polymerization, where poly (acrylic acid) is produced independently of the cellulose backbone. This will reduce the grafting and thus the loading [38].

Table 5: L_{max} (%) and EL(%) of the hydrogel loaded with KNO_3

Hydrogel	L_{max} (%)	EL (%)
MC-g-AA/MBA	19.3	38.61

Release of KNO_3 from loaded microspheres

The release behaviors of the loaded fertilizer on the manufactured hydrogels were tested under different pH circumstances of the release media. The release of 100 mg loaded microspheres of fertilizer was allowed to occur in 20 ml of different pH buffered solutions (pH 4, pH 7 and pH 9) made in rainwater and at 45°C. The λmax for KNO_3 fertilizer was fixed at 298 nm using a UV-visible spectrophotometer, and at intervals of 2 hours, a sample (3 mL) was collected from the release medium, and its absorbance was measured by UV. The release percentage (BRmax % and CRmax %) (Eqs. 4 and 5) of KNO_3 was estimated by using the measured absorbance (A) of the unknown KNO_3 against its typical calibration curve to find its release concentration at each time interval.

Table 6: Cumulative release Rcum (wt%) (Eq. 6) of KNO_3 from (MC-g-AA)/MBA hydrogel in three different pHs

Hydrogel	L_{max} (%) KNO_3	Rcum (wt%) KNO_3		
		pH4	pH7	pH9
MC-g-AA/MBA	19.30	16.83	18.81	16.83

The release profile of KNO_3-loaded (MC-g-AA)/MBA copolymer hydrogel (Fig. 15, and Table 6) is found to be more regular and regulated at pH 7, where poly (acrylic acid) chains are ionized at neutral pH. The ionization of AA chains enhances the electrostatic repulsion, which widens the hydrogel network and promotes a diffusion-controlled release of the hydrogel [39].

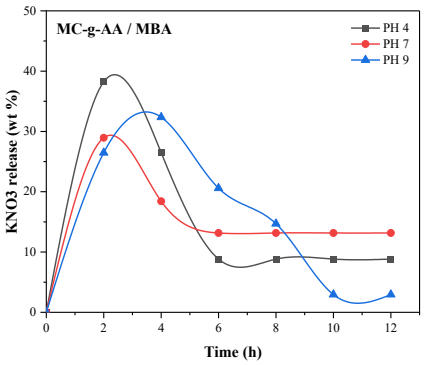

Figure 15: Weight percent of burst release (BRmax %) and controlled release (CRmax %) of (MC-g-AA)/MBA hydrogel versus time (h) in different pHs

Water Retention Study

The hydrogel employed for water retention is that of high degree swelling measurement (CE-g-AA)/MBA. The study involves studying soil saturation with water and then water retention in soil. The estimation of the degree of saturation of the agricultural soil sample (g / g) using Eq. 7, and the outcome was as follows:

Degree of soil saturation (g/g) = $\frac{W_a - W_o}{W_o} = \frac{220-150}{150}$ = 0.47 g water/g of soil was added to the water retention tested samples.

The water retention (g/g) was determined according to Eq. 8, by using the weight reading each day for soil with hydrogel samples and the control sample. The samples were stored under managed temperature ranges (35-40) ℃ and humidity (40 %). The addition of superabsorbent hydrogel to the soil can greatly improve water retention and at the same time reduce water evaporation. The water retention results were drawn in (Fig. 16 and Table 7), showing characterization of the hydrogel in retaining water inside the agricultural soil compared to the control sample. Water was added to the hydrogel to allow it to swell and reach its maximum swelling rate before being added to agricultural soil, followed by the addition of a fixed amount of water to the sample. In Table 7, we can see that the starting weight of the sample differs depending on the control. Otherwise, the weight of the sand and water added is the same for both the sample and the control. The tested samples display various characteristics in quantities and the number of days to retain water within the form. The control model retained water for thirteen days and then stabilized in weight to a dry condition (Fig. 16, Table 7).

Table 7: Daily decrease in the weight of soil for hydrogel and control samples

Time (Day)	Decrease in the weight of sample (g)	
	Control	(CE-g-AA) /MBA hydrogel
1	226.16	238.55
2	220.39	232.01
3	211.11	222.90
4	203.26	215.33
5	196.36	207.82
6	189.90	201.20
7	182.30	194.64
8	177.40	188.62
9	171.11	182.61

10	166.70	177.58
11	163.20	172.30
12	159.52	167.60
13	155.40	164.30
14		162.21
15		160.40
16		158.70
17		157.60
18		156.66
19		156.35

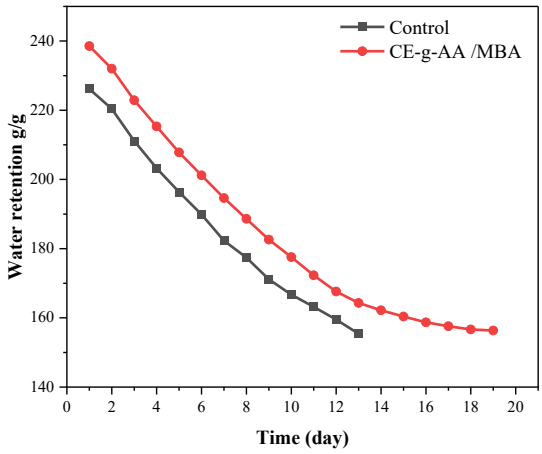

Figure 16: Effect of superabsorbent hydrogel added to the agricultural soil on water retention (g/g) versus time (day) compared to control

The 3D porous structure of the hydrogel, along with electrostatic repulsion and the high-water affinity of its chemical groups that extend the polymer network of (CE-g-AA/MBA) hydrogel, is responsible for the long-term retention of water compared to the control sample. Both cellulose (-OH) and grafted AA (-COOH) groups form strong hydrogen bonds with water molecules due to their hydrophilic functional groups. The hydrogen bonds linking the water molecules to the matrix effectively limit the evaporation rate. The MBA cross-linker covalently links the polymer chains to an insoluble network. The cross-linked hydrogel structure is responsible for swelling without dissolving, does not readily leak water under pressure, and also provides the required elasticity [35].

CONCLUSIONS

Two hydrogels have been developed for agricultural use in the field of agrochemical-controlled delivery systems includes fertilizers to plants, as well as for the purpose of watering plants and retaining water for the longest regular period. Through the investigations, two hydrogels were prepared from cellulose and methylcellulose and grafted with acrylic acid and cross-linked with MBA. The hydrogel (CE-g-AA)/MBA was found suitable for water retention because of its high swelling and it actually showed this by retaining water in the soil for a long period of time, and at the same time reduce water evaporation. Whereas, the hydrogel (MC-g-AA)/MBA was demonstrate high viability by loading nitrogen fertilizer model KNO_3, holding it, and then releasing it in different pHs media. The KNO_3 fertilizer was released regularly and for a long release period in pH 7 medium, where acrylic acid chains ionization increases electrostatic repulsion and facilitates a diffusion- controlled release of the hydrogel.

Acknowledgements: The authors acknowledge chemistry department, university of Mosul for supporting and guiding the work.

Author Contributions: The author Fawzi H. Jabrail contributed to the methodology, supervised the work. The author Akram W. Nayyef was responsible for hydrogels preparation, data collection and investigations. Both authors have read and approved the final manuscript.

Conflict of Interest: The authors declare no conflict interests.

REFERENCES

[1] Piccoli I, Camarotto C, Squartini A, et al. Hydrogels for agronomical application: from soil characteristics to crop growth: a review. Agron Sustain Dev. 2024; 44: 22. DOI: 10.1007/s13593-024-00958-4

[2] Tariq Z, Iqbal DN, Rizwan M, et al. Significance of biopolymer-based hydrogels and their applications in agriculture. RSC Adv. 2023; 13: 24731-24754. DOI: 10.1039/D3RA03472K.

[3] Yu L, Gao X, Zhao X. Global synthesis of the impact of droughts on crops' water-use efficiency (WUE): Towards both high WUE and productivity. Agric Syst. 2020; 177: 102723. DOI: 10.1016/j.agsy.2019.102723.

[4] Zowada R, Foudazi R. Macroporous hydrogels for soil water retention in arid and semi-arid regions. *RSC Applied Polymers*. 2023; 1:243-253. DOI: 10.1039/D3LP00117B.

[5] Granados-Carrera CM, Perez-Puyana VM, Jiménez-Rosado M, Romero A. Hydrogel Development, Processing and Applications in Agriculture: A Review. *Gels*. 2026;12(3):259. DOI: 10.3390/gels12030259.

[6] Azeem B, Rasool A, Qureshi MAU, et al. Eco-friendly three-dimensional hydrogels for sustainable agricultural applications: Current and future scenarios. *Polymers for Advanced Technologies*. 2023;34(10):3287-3314. DOI: 10.1002/pat.6122.

[7] Wu C, Li J, Zhang YQ, Li X, Wang SY, Li DQ. Cellulose Dissolution, Modification, and the Derived Hydrogel: A Review. ChemSusChem. 2023;16(21). DOI: 10.1002/cssc.202300518.

[8] El Idrissi A, Channab B, Essamlali Y, Zahouily M. Superabsorbent hydrogels based on natural polysaccharides: Classification, synthesis, physicochemical properties, and agronomic efficacy under abiotic stress conditions: A review. *International Journal of Biological Macromolecules*. 2024;258(Part 2):128909. DOI: 10.1016/j.ijbiomac.2023.128909.

[9] Zhu J, Zhang Z, Wen Y, Song X, Tan WK, Ong CN, Li J. Recent Advances in Superabsorbent Hydrogels Derived from Agro Waste Materials for Sustainable Agriculture: A Review. *Journal of Agricultural and Food Chemistry*. 2024;72(41):22399-22419. DOI: 10.1021/acs.jafc.4c04970.

[10] Tofanica BM, Mikhailidi A, Samuil C, Ungureanu OC, Fortună ME, Ungureanu E. Advances in Cellulose-Based Hydrogels: Current Trends and Challenges. *Gels*. 2024;10(12):842. DOI: 10.3390/gels10120842.

[11] Pang L, Gao Z, Feng H, Wang S, Wang Q. Cellulose based materials for controlled release formulations of agrochemicals: A review of modifications and applications. J Control Release. 2019; 316: 105-115. DOI: 10.1016/j.jconrel.2019.11.004.

[12] Jabrail FH, Mutlaq MS, Al-Ojar RK. Studies on agrochemical-controlled release behavior of copolymer hydrogel with PVA blends of natural polymers and their water-retention capabilities in agricultural soil. Polymers. 2023;15(17):3545. DOI: 10.3390/polym15173545.

[13] Lakhani KG, Salimi M, Idrissi AE, et al. Nanocellulose-hydrogel hybrids: synthesis and applications in agriculture. Int J Biol Macromol. 2025; 309: 143081. DOI: 10.1016/j.ijbiomac.2025.143081.

[14] Saberi Riseh R, Vazvani MG, Hassanisaadi M, Skorik YA. Micro-/Nano-Carboxymethyl Cellulose as a Promising Biopolymer in Agriculture. Polymers. 2023; 15: 440. DOI: 10.3390/polym15020440.

[15] Dutta SD, Patel DK, Lim KT. Functional cellulose-based hydrogels as extracellular matrices for tissue engineering. J Biol Eng. 2019; 13: 55. DOI: 10.1186/s13036-019-0177-0.

[16] Altynov Y, Bexeitova K, Nazhipkyzy M, et al. Nanocellulose hydrogels from agricultural wastes. Nanoscale. 2025; 17: 12580-12619. DOI: 10.1039/D5NR00997A.

[17] Anuar WAN, Ramli RA, El-Sayed MM, Warkar SG. Recent study on biodegradable hydrogels for agriculture application: A review. *Journal of Environmental Chemical Engineering*. 2025;13(2):115679. DOI: 10.1016/j.jece.2025.115679.

[18] Tang Y, Fang Z, Lee HJ. Exploring Applications and Preparation Techniques for Cellulose Hydrogels: A Comprehensive Review. *Gels*. 2024;10(6):365. DOI: 10.3390/gels10060365.

[19] Omidian H, Akhzarmehr A, Dey Chowdhury S. Advancements in Cellulose-Based Superabsorbent Hydrogels: Sustainable Solutions across Industries. *Gels.* 2024;10(3):174. DOI: 10.3390/gels10030174.
[20] Priya AS, Premanand R, Ragupathi I, Bhaviripudi VR, Aepuru R, Kannan K, Shanmugaraj K. Comprehensive Review of Hydrogel Synthesis, Characterization, and Emerging Applications. *Journal of Composites Science.* 2024;8(11):457. DOI: 10.3390/jcs8110457.
[21] 21.AL-Ojar RK, Jabrail FH. Release behavior of bovine serum albumin loaded on hydrogels of natural polymer blend poly (vinyl alcohol) and analyze their compositions. Amer. J. Polym. Sci. Tech. 2019;5(2), 40-54.
[22] Gupta KC, Jabrail FH. Glutaraldehyde cross-linked chitosan microspheres for controlled release of centchroman. Carbohy. Res., 2007;342, 2244-2252.
[23] AL-Omari AFS, Jabrail FH. Chitosan/starch-based hydrogels as drug delivery carrier for controlled release of hydroxychloroquine. J. Chem. Health Risks. 2023;13(3), 1457-1471.
[24] Raheem DJ, Sadraddin AS, Jabrail FJ. Comparative design and evaluation of chitosan hydrogels grafted with itaconic acid-alginate for enhanced linagliptin delivery. J. Appl. Polym. Sci. 2026;143: e70903.
[25] 25.Nayyef AW, Jabrail FH. Synthesis and characterization of poly (ethylene glycol)-based hydrogels reinforced with different cross-linkers for regulating the release of nitrogen fertilizer. 2026;30(5), 2605-2624.
[26] Jabrail FH, Mahmood ME. Hydrophilic monomers graft gum Arabic hydrogels prepared in different cross-linking nature and study of their effects on irrigation of agriculture soil. Res. J. Chem. Sci. 2016; 6(1), 1-19.
[27] Mutlaq MS, Jabrail FH. Controlled delivery system for NPK agrochemical release from chitosan copolymer hydrogels. Amer. J. Appli. Sci., 2022;19, 84-92.
[28] Zou P, Yao J, Cui YN, Zhao T, Che J, Yang M, Li Z, Gao Y. Advances in cellulose-based hydrogels for biomedical engineering. Gels. 2022;8(6):364. doi:10.3390/gels8060364.
[29] Niemczyk-Soczynska B, Gradys A, Kolbuk D, Krzton-Maziopa A, Rogujski P, Stanaszek L, et al. A methylcellulose/agarose hydrogel as an innovative scaffold for tissue engineering. RSC Adv. 2022;12(41):26882-26894.
[30] Saragih SW, Wirjosentono B, Meliana Y. Influence of crosslinking agent on the morphology, chemical, crystallinity and thermal properties of cellulose nanofiber using steam explosion. Case Stud Therm Eng. 2020; 22: 100740.
[31] Fahad M, Khan MA, Gilbert M. Investigation of thermal gel formation of methylcellulose in glycols using DSC and XRD. Gels. 2021;7(4):205.
[32] 32 .Cuccia NL, Pothineni S, Wu B, Méndez Harper J, Burton JC. Pore-size dependence and slow relaxation of hydrogel friction on smooth surfaces. Proc Natl Acad Sci U S A. 2020;117(21):11247-11256.
[33] 33 .Tolentino MK, Du EY, Silvani G, Pandzic E, Kilian KA, Gooding JJ. Decoding hydrogel porosity: advancing the structural analysis of hydrogels for biomedical applications. Adv Healthc Mater. 2025;14(22):2500658.
[34] Bhuyan MM, Jeong JH. Preparation of hydrogels by cross-linking and multidimensional applications. Gels. 2025;11(11):896. doi:10.3390/gels11110896.
[35] Rizwan M, Gilani SR, Durani AI, Naseem S. Materials diversity of hydrogel: Synthesis, polymerization process and soil conditioning properties in agricultural field. J. Adv. Res. 2021; 33: 15-40.
[36] Han Z, Zhu H, Cheng JH. Novel double cross-linked acrylic acid/bagasse cellulose porous hydrogel for controlled release of citral and bacteriostatic effects. ACS Appl Mater Interfaces. 2023;15(16):20358-20371. doi:10.1021/acsami.3c00289.
[37] Gala S, Mao Y, Bao X, Pan YF, Huang JT. Preparation of high water-absorbing hydrogel based on grafted micro/nano cellulose. BioResources. 2021;16(1):1256.
[38] Noordergraaf IW, Witono JR, Heeres HJ. Grafting starch with acrylic acid and Fenton's initiator: The selectivity challenge. Polymers. 2024;16(2):255. doi:10.3390/polym16020255.
[39] Ureña-Amate MD, Socias-Viciana MM, Urbano-Juan MM, García-Alcaraz MC. Effects of pH and crosslinking agent in the evaluation of hydrogels as potential nitrate-controlled release systems. Polymers. 2023;15(5):1246.